


RESEARCH ARTICLE

Modeling the spatiotemporal dynamics of industrial sulfur dioxide emissions in China based on DMSP-OLS nighttime stable light data

Yanlin Yue¹ , Zheng Wang^{1,2*}, Li Tian³, Jincal Zhao⁴, Zhizhu Lai¹, Guangxing Ji¹, Haibin Xia¹

1 Key Laboratory of Geographic Information Science, Ministry of Education, East China Normal University, Shanghai, China, **2** Institute of Science and Development, Chinese Academy of Sciences, Beijing, China, **3** Jinan Experimental School of East China Normal University, Jinan, Shandong, China, **4** School of Business, Henan Normal University, Xinxiang, Henan, China

* wangzheng@casipm.ac.cn



OPEN ACCESS

Citation: Yue Y, Wang Z, Tian L, Zhao J, Lai Z, Ji G, et al. (2020) Modeling the spatiotemporal dynamics of industrial sulfur dioxide emissions in China based on DMSP-OLS nighttime stable light data. PLoS ONE 15(9): e0238696. <https://doi.org/10.1371/journal.pone.0238696>

Editor: Min Huang, George Mason University, UNITED STATES

Received: November 7, 2019

Accepted: August 22, 2020

Published: September 10, 2020

Copyright: © 2020 Yue et al. This is an open access article distributed under the terms of the [Creative Commons Attribution License](https://creativecommons.org/licenses/by/4.0/), which permits unrestricted use, distribution, and reproduction in any medium, provided the original author and source are credited.

Data Availability Statement: All relevant data are within the manuscript and its Supporting Information files.

Funding: This work was supported by National Key Research and Development Program of China [Grant Number: 2016YFA0602703], National Natural Science Foundation of China [Grant Number: 41671396], and Natural Science Foundation of Shanghai, China [Grant Number: 19ZR1415200].

Abstract

Due to the rapid economic growth and the heavy reliance on fossil fuels, China has become one of the countries with the highest sulfur dioxide (SO₂) emissions, which pose a severe challenge to human health and the sustainable development of social economy. In order to cope with the serious problem of SO₂ pollution, this study attempts to explore the spatial temporal variations of industrial SO₂ emissions in China utilizing the Defense Meteorological Satellite Program's Operational Linescan System (DMSP-OLS) nighttime stable light (NSL) data. We first explored the relationship between the NSL data and the statistical industrial SO₂ emissions at the provincial level, and confirmed that there was a positive correlation between these two datasets. Consequently, 17 linear regression models were established based on the NSL data and the provincial statistical emissions to model the spatial-temporal dynamics of China's industrial SO₂ emissions from 1997 to 2013. Next, the NSL-based estimated results were evaluated utilizing the prefectural statistical industrial SO₂ emissions and emission inventory data, respectively. Finally, the distribution of China's industrial SO₂ emissions at 1 km spatial resolution were estimated, and the temporal and spatial dynamics were explored from multiple scales (national scale, regional scale and scale of urban agglomeration). The results show that: (1) The NSL data can be successfully applied to estimate the dynamic changes of China's industrial SO₂ emissions. The coefficient of determination (R²) values of the NSL-based estimation results in most years were greater than 0.6, and the relative error (RE) values were less than 10%, when validated by the prefectural statistical SO₂ emissions. Moreover, compared with the inventory emissions, the adjusted coefficient of determination (Adj.R-Square) reached 0.61, with the significance at the 0.001 level. (2) During the observation period, the temporal and spatial dynamics of industrial SO₂ emissions varied greatly in different regions. The high growth type was largely distributed in China's Western region, Central region, and Shandong Peninsula, while the no-obvious-growth type was concentrated in Western region, Beijing-Tianjin-Tangshan and Middle south of Liaoning. The high grade of industrial SO₂ emissions was mostly concentrated in

Competing interests: The authors have declared that no competing interests exist.

China's Eastern region, Western region, Shanghai-Nanjing-Hangzhou and Shandong Peninsula, while the low grade mainly concentrated in China's Western region, Middle south of Liaoning and Beijing-Tianjin-Tangshan. These results of our research can not only enhance the understanding of the spatial-temporal dynamics of industrial SO₂ emissions in China, but also offer some scientific references for formulating feasible industrial SO₂ emission reduction policies.

Introduction

Sulfur dioxide (SO₂) is one of the main pollutants in the atmosphere, which is an important indicator to measure whether the atmosphere is polluted [1]. SO₂ is released when burning materials containing sulfur, which is found in all types of coal and oil across the world in varying proportions. As an acidic and toxic gas, SO₂ leads to global acid rain, visibility degradation, destruction of terrestrial and aquatic ecosystems and dangerous impacts on the human health [2–6]. In brief, it causes serious losses to the whole society and the economy. SO₂ in the atmosphere can be emitted from both natural and anthropogenic sources [7]. Natural SO₂ sources mainly come from oxidation of biogenic dimethyl sulfide and volcanic eruption [8]. While, the primary anthropogenic SO₂ emission is from fossil fuel consumption, especially for power generation, and other industrial production activities [9]. It is estimated that anthropogenic emissions are the main source of global SO₂ emissions [10, 11].

China is one of the countries with the highest SO₂ emissions [12] and the largest area exposed to acid precipitation in the world [13], because its huge economy relies heavily on fossil fuels as an energy source [14]. In 2015, China emitted 18.591 million tons of SO₂, of which 83.73% was industrial SO₂ [15]. In order to reduce SO₂ emission to mitigate the adverse impacts, a range of measures has been advanced by the Chinese government, including installing flue gas desulfurization on facilities power plants [16], increasing the proportion of non-fossil fuels [17], and carrying out a plan that the SO₂ emission in 2020 shall reduce by 15% compared with 2015 [18]. Although the Chinese government has made tremendous efforts to control the air quality, the current situation of air pollution is still not optimistic, as for the air quality in many cities still could not meet the national air quality standards [19]. For instance, in 2017, only 99 out of the 338 cities in China met the environmental air quality standards, while 70.7% failed to achieve the national air quality standards [20]. More seriously, SO₂ can affect the atmosphere and environment on a global scale [21, 22]. It means that studying on SO₂ emissions in China is also of great significance to improve global environmental performance. Therefore, it is urgently necessary to explore the dynamic characteristics of SO₂ emissions in China, for obtaining a better understanding of the current air pollution situation and formulating appropriate emission reduction policies.

Remote sensing can provide valuable data sources in the research of detecting the spatial and temporal changes of geospatial information. Numerous literatures have proved that DMSP-OLS nighttime light imagery can perform well in the detection of socioeconomic activities, such as, monitoring urban dynamics [23–26], measuring spatial distribution of population [27–30], investigating economic development [31–33], estimating power energy consumption [34–37], etc. The significant correlation between the DMSP-OLS NSL data and energy consumption has been verified [38, 39], and the NSL data has been successfully applied to fossil fuel related CO₂ emissions [40–44] and pollutant emissions (such as PM_{2.5} emissions and nitrogen oxides emissions) [45–50]. For instance, Ghosh et al. [41] applied nighttime

satellite imagery favorably to map fossil fuel CO₂ emissions. Li et al. [45] utilized nighttime light imagery to PM_{2.5} pollution estimation in Beijing using an established model and the average precision of the estimation reached 0.796. Xu et al. [46] taking Shanghai, China as an example, verified the effectiveness of DMSP nighttime light images in predicting urban daily PM_{2.5} concentrations. Toenges-Schuller et al. [47] employed DMSP-OLS nighttime light images for detecting the global distribution patterns of anthropogenic nitrogen oxides emission. Jiang et al. [48] quantified the spatial-temporal dynamics of nitrogen oxides emissions in China utilizing a NSL based model. In summary, DMSP-OLS NSL data has been proved to be promising in monitoring fossil fuel related CO₂ emissions and pollutant emissions. As anthropogenic SO₂ emissions are mainly from fossil fuel combustion [51, 52], thus, there is a good potential to estimate industrial SO₂ emissions based on NSL data. Moreover, existing researches have also demonstrated that there was a significant correlation between nighttime light data and gross domestic product of secondary industry [53, 54]. Therefore, theoretically, the industrial SO₂ emissions can also be estimated utilizing nighttime light data. In addition, different from the bottom-up emission inventories which are usually highly uncertain and not timely updated [55], NSL data can provide spatial explicit images with high resolution in time. But there are few studies about whether and how the NSL data could be applied to estimate the spatial-temporal dynamics of industrial SO₂ emissions. Hence, we tried to apply the nighttime light data to estimate industrial SO₂ emissions in China.

This study aims to test the utility of modeling the spatiotemporal dynamics changes of China's industrial SO₂ emission based on DMSP-OLS nighttime stable light data. Specifically, the major objectives of our study are: (1) confirming a positive correlation was truly existed between the industrial sulfur dioxide emissions and DMSP-OLS NSL data, (2) building models to investigate China's industrial SO₂ emission utilizing the NSL data, and evaluating the estimation accuracy using statistical emissions and emission inventory data, respectively, (3) exploring the spatiotemporal distribution characteristics of China's industrial SO₂ emission from three different scales on the basis of the NSL-based estimation results, and putting forward some suggestions on industrial SO₂ emission mitigation, accordingly.

Study area and data

Study area

In order to learn more about the spatiotemporal variations and changes of industrial SO₂ emissions in China for 1997–2013, the research area was determined by three different administrative levels (Fig 1). National scale is the first administrative level. In recent years, a vast volume of SO₂ emitted from industrial production has brought about serious atmospheric pollution. It is necessary to explore the overall situation of industrial SO₂ emissions in the whole country firstly. Considering that the statistical industrial SO₂ emissions data was absent in some areas (Hong Kong, Macao and Taiwan), the first level was limited to mainland China. Then, regional scale is the second level. Because of the imbalanced socioeconomic development in our country, great disparities of industrial SO₂ emissions within different economic regions have been formed. In order to reveal the differences among regions, we divided the research area into four regions according to its geographical position and socioeconomic development level. So, Eastern region, Central region, Western region and Northeastern region were studied separately. Finally, the scale of urban agglomeration is the third administrative level. As far as we know, the population and economic growth of China were mainly concentrated in urban agglomerations, these areas contributed more to industrial SO₂ emissions in the whole country. Consequently, it is of great significance to explore the characteristic of industrial SO₂ emissions in urban agglomerations for reducing SO₂ pollution. Therefore, six representative urban

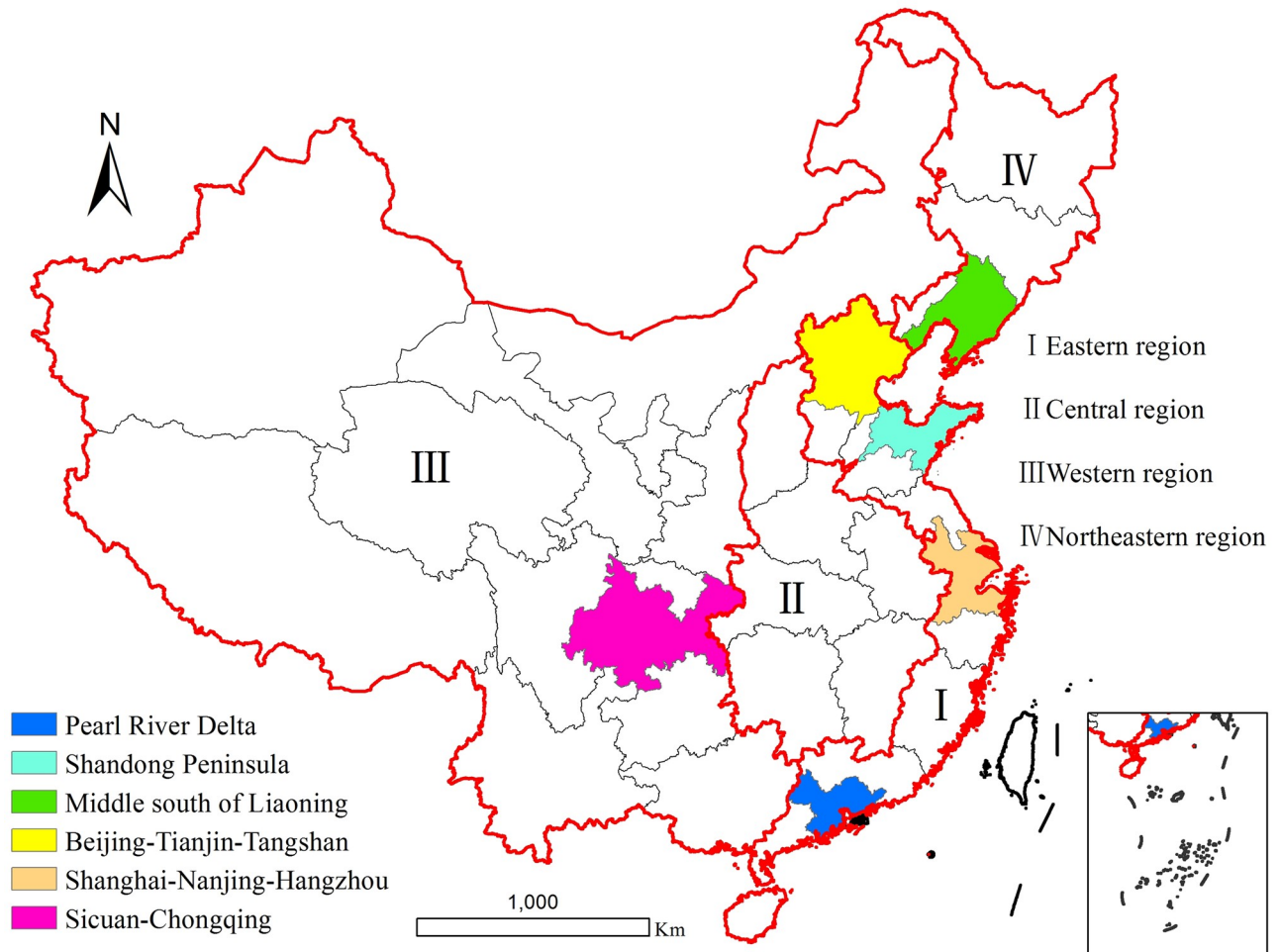


Fig 1. Study area.

<https://doi.org/10.1371/journal.pone.0238696.g001>

agglomerations were finally chosen as the third level, namely Middle south of Liaoning, Beijing-Tianjin-Tangshan, Shandong Peninsula, Pearl River Delta, Sichuan-Chongqing and Shanghai-Nanjing-Hangzhou.

Data

There are mainly two kinds of data sets utilized in this research, namely, DMSP-OLS NSL data and statistical industrial SO₂ emissions data. NSL data from 1997 to 2013 were derived from the National Oceanic and Atmospheric Administration's National Geophysical Data Center (NOAA/NGDC) website (<http://www.ngdc.noaa.gov/eog/dmsp/downloadV4composites.html>). These NSL images measured lights on the Earth's surface from human settlements, road networks and other sites with continuous lighting. The digital number (DN) value of the NSL imagery ranges from 0 to 63. And, the spatial resolution of the NSL images is 0.0083° (about 1 km). Due to the following two shortcomings of DMSP-OLS NSL data: (1) pixel saturation effect and (2) discontinuity and incomparability phenomenon, it is necessary to intercalibrate the data before using it. In order to intercalibrate the NSL data, Shi et al. [37] developed a modified invariant region (MIR) method, consisting of reduction of saturation effect and

correction of discontinuity effect. In our study, the time series NSL data were directly intercalibrated based on the specific equations and parameters reported in the article of Shi et al.

Additionally, statistical data of industrial SO₂ emissions including provincial statistics and prefectural statistics were derived from Statistical Yearbooks of different provinces (1998–2014) and China City Statistical Yearbook (2004, 2005, 2009, 2010, 2013 and 2014). In detail, the provincial statistics emissions were used for modeling the industrial SO₂ emissions at 1km resolution, while the prefectural statistics emissions were used to assess the accuracy of simulation. The industrial SO₂ emission data can be found in the [S1](#) and [S2](#) Files in the Supporting information section.

Methodology

For investigating the spatial-temporal dynamics of China's industrial SO₂ emissions, main research procedures include: (1) correlation analysis between nighttime light images and statistical industrial SO₂ emissions at the provincial level; (2) estimation of industrial SO₂ emissions at 1 km resolution based on NSL data and provincial statistics emissions; (3) accuracy assessment of industrial SO₂ emissions estimation by prefectural statistical emission data and emission inventory data; (4) multiscale analysis of the spatiotemporal characteristics of industrial SO₂ emissions.

Correlation analysis

Correlation analysis was employed to analyze whether there exists a significant correlation between DMSP nighttime light images and statistical industrial SO₂ emissions or not. The formulas we used for correlation analysis can be represented as follows:

$$r_{xy} = \frac{\sum_{k=1}^n (x_k - \bar{x})(y_k - \bar{y})}{\sqrt{\sum_{k=1}^n (x_k - \bar{x})^2 \sum_{k=1}^n (y_k - \bar{y})^2}} \quad (1)$$

$$\bar{x} = \frac{1}{n} \sum_{k=1}^n x_k \quad (2)$$

$$\bar{y} = \frac{1}{n} \sum_{k=1}^n y_k \quad (3)$$

Where, r_{xy} is expressed as the degree of correlation between variable x and variable y , whose value ranges from -1 to 1. And the closer absolute value of r_{xy} is to 1, the stronger correlation between x and y is. In this paper, variables x and y represent DN values of DMSP nighttime light images and industrial SO₂ emissions, respectively.

Estimation of industrial SO₂ emissions

Once the significant positive correlation between NSL data and statistical industrial SO₂ emissions data is confirmed, industrial SO₂ emission at the provincial level can be simulated using NSL data. Then, the linear regression model was performed to estimate industrial SO₂ emissions, and the equation can be described as the following:

$$S_p = a \times TNSL + b \quad (4)$$

Where S_p stands for the provincial industrial SO₂ emissions, TNSL represents the total night-time stable light values of each province, a is the regression coefficient, and b stands for the intercept.

Considering the absence of industrial SO₂ emissions at the pixel level, the positive correlation between NSL data and industrial SO₂ emissions is assumed to be constant within the same province. Additionally, provincial statistical industrial SO₂ emissions data were employed to correct the estimation models to reduce the error within a provincial unit. The formula is:

$$CS_i = SS_p \times (S_i \div TS_p) \tag{5}$$

Where CS_i indicates the corrected industrial SO₂ emissions of the i pixel; SS_p stands for the statistical industrial SO₂ emissions of the p province; S_i is the estimated industrial SO₂ emissions of the i pixel; TS_p represents the estimated industrial SO₂ emissions of the p province.

Accuracy assessment of industrial SO₂ emissions estimation

It is necessary and crucial to assess the accuracy of industrial SO₂ emissions estimation. Two indicators, the coefficient of determination (R^2), and the relative error (RE) were often used to assess the accuracies of simulated results [56, 57]. For instance, Shi et al. [37] modeled the spatiotemporal dynamics of global electric power consumption by DMSP-OLS NSL data, and 128 samples of country-level statistical electric power consumption data from 1992 to 2012 were collected to calculate the R^2 and RE which were employed to evaluate the estimation accuracy.

To validate the accuracy of industrial SO₂ estimation models, R^2 , and RE are calculated:

$$R^2 = \frac{\sum_{c=1}^m (S_c - \overline{SS_c})^2}{\sum_{c=1}^m (SS_c - \overline{SS_c})^2} \tag{6}$$

$$RE = \frac{S_c - SS_c}{SS_c} \tag{7}$$

Where, m is the total number of validation regions which was set to 263 in our research, SS_c stands for the statistical industrial SO₂ emissions of the c city, $\overline{SS_c}$ indicates the average of SS_c , S_c is the estimated industrial SO₂ emissions of the c city. In the above three parameters, the higher R^2 value and the lower absolute RE values indicate a higher simulation accuracy.

Evaluation of spatiotemporal dynamics of industrial SO₂ emissions

First of all, the average industrial SO₂ emissions from 1997 to 2013 was calculated using the following equation to analyze the spatial pattern of industrial SO₂ emissions:

$$\overline{S}_i = \frac{\sum_{n=1997}^{2013} S_i}{t} \tag{8}$$

Where \overline{S}_i stands for the average industrial SO₂ emissions in pixel i for 1997–2013, and t indicates the total number of years which was set to 17 in our research.

Next, the temporal variation of industrial SO₂ emissions between 1997 and 2013 can be described by the following formula:

$$S_i^{tem} = S_i^{2013} - S_i^{1997} \tag{9}$$

Where S_i^{tem} stands for the temporal variation of industrial SO₂ emissions in pixel i from 1997 to 2013.

Then, the Natural Break method, which can maximize the differences between classes with no effect of human factors [58], was used for investigating the spatial and temporal changes of industrial SO₂ emissions in China. In detail, the spatial variation map of industrial SO₂ emissions was divided into five grades: low (< 3 t), relatively low (3–15 t), medium (14–37 t), relatively-high (37–70 t) and high (> 70 t). And, the temporal variation of China's industrial SO₂ emissions was sorted into 4 types: no-obvious-growth (< 2t), low growth (2–9 t), moderate-growth (9–22 t), and high growth (> 22 t).

Results

Correlation analysis results

The relationship between the DMSP nighttime light imagery and industrial SO₂ emissions for 1997–2013 was confirmed utilizing the formulas as described in Section 3.1. And the correlation coefficients between the two from 1997 to 2013 were listed in Table 1. Obviously, the correlation coefficients over the observation period are all greater than $r_{0.001} = 0.5974$, which demonstrated that the correlation between these two datasets was significant at the level of $\alpha = 0.001$. Based on this, 17 liner regression models were constructed to estimate industrial SO₂ emissions. And the F values of these models are all greater than $F_{0.005}(1, 29) = 9.23$, revealing a statistical significance at the level of $\alpha = 0.005$.

Spatiotemporal dynamics of industrial SO₂ emissions for 1997–2013. The spatial-temporal variations of China's industrial SO₂ emissions during the period of 1997–2013 was mapped in Fig 2. In terms of spatial distribution, industrial SO₂ emissions in China were mainly concentrated in the eastern half of the country. Specifically, the high industrial SO₂ emissions were clearly identified in some economically developed cities like Yangtze River Delta, Sichuan-Chongqing, and Pearl River Delta and Huang-Huai-Hai region. While, the low

Table 1. Correlation analysis results.

Year	Correlation coefficient	F value
1997	0.718	30.84
1998	0.731	33.37
1999	0.714	30.20
2000	0.713	30.03
2001	0.755	38.54
2002	0.762	40.25
2003	0.728	32.72
2004	0.742	35.62
2005	0.761	39.91
2006	0.730	33.04
2007	0.741	35.28
2008	0.747	36.63
2009	0.743	35.83
2010	0.747	36.68
2011	0.738	34.64
2012	0.743	35.81
2013	0.720	31.22

<https://doi.org/10.1371/journal.pone.0238696.t001>

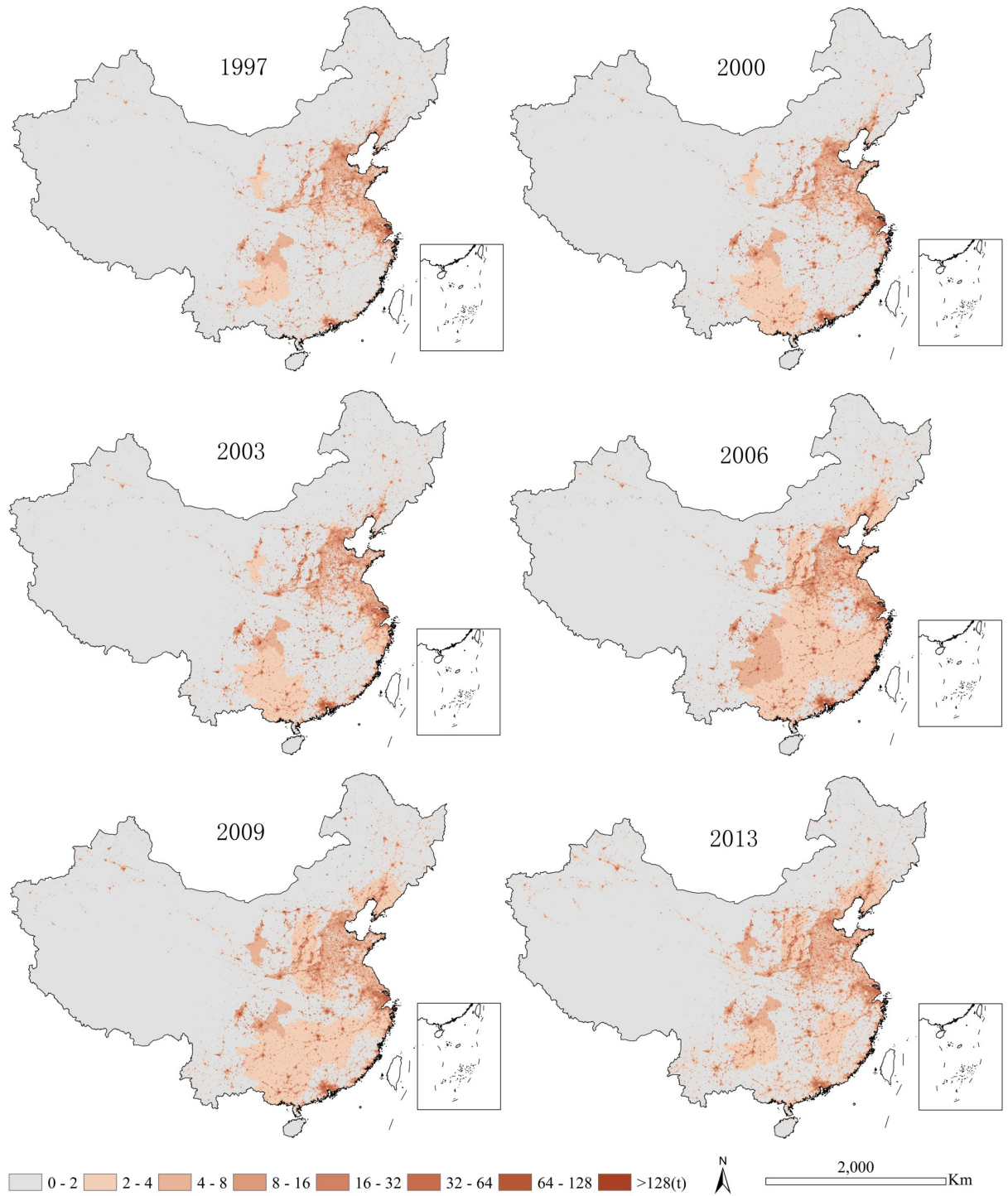


Fig 2. Maps of China’s industrial SO₂ emissions for 1997–2013.

<https://doi.org/10.1371/journal.pone.0238696.g002>

industrial SO₂ emissions were largely distributed in the western and northeastern China. In terms of the temporal variations, China’s industrial SO₂ emissions increased significantly in the initial period from 1997 to 2013 and then slowly decreased. Overall, the temporal and spatial changes of industrial SO₂ emissions in China are significant.

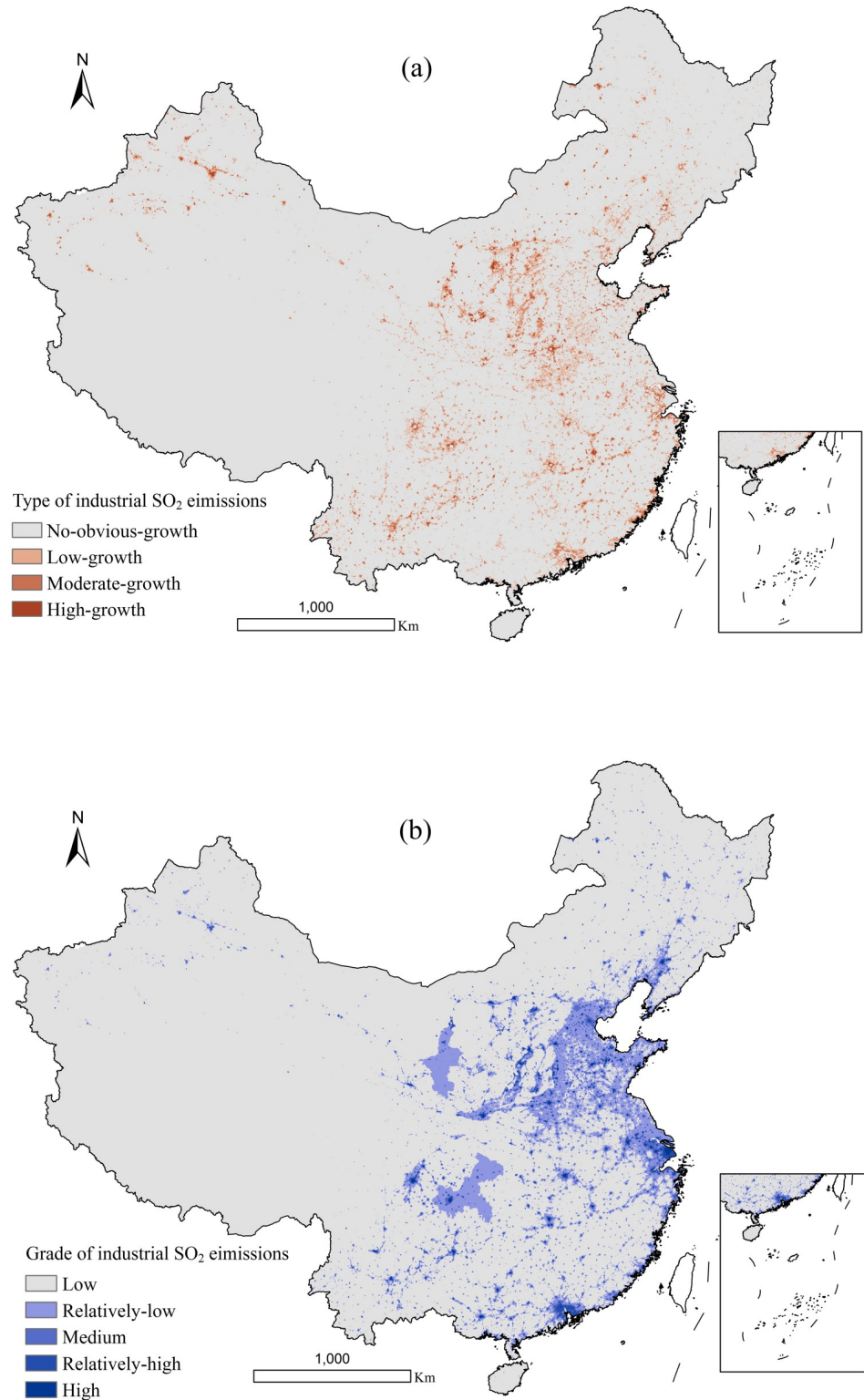


Fig 3. Temporal variations (a) and spatial variations (b) of China's industrial SO₂ emissions for 1997–2013. The non-positive growth was regarded as no-obvious growth.

<https://doi.org/10.1371/journal.pone.0238696.g003>

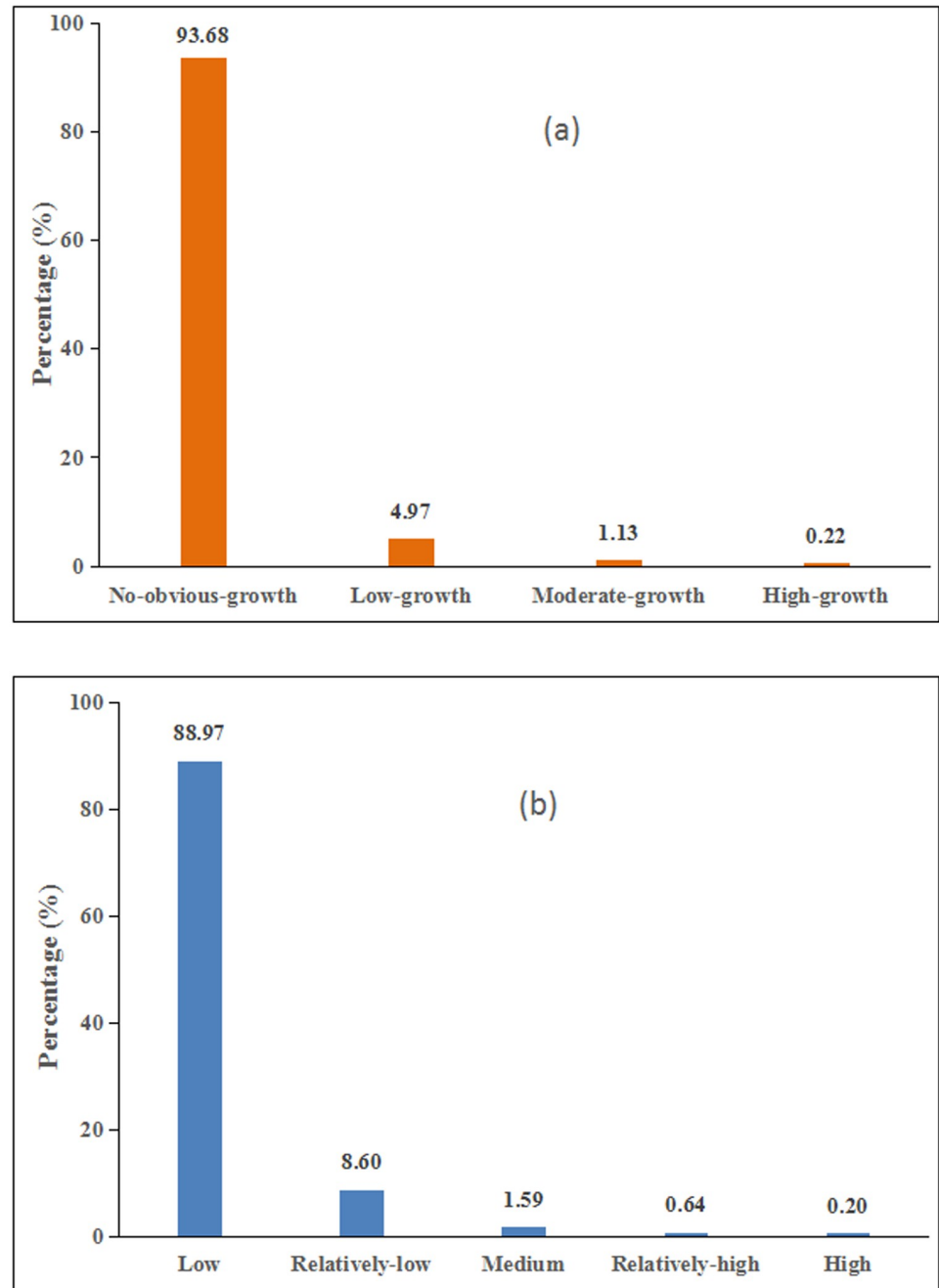


Fig 4. Areal percentage of each type (a) and each grade (b) in China.

<https://doi.org/10.1371/journal.pone.0238696.g004>

Spatiotemporal dynamics of industrial SO₂ emissions at national scale. Fig 3a showed the spatial distribution of the four types, which reflected the temporal variations of industrial SO₂ emissions during the period of 1997–2013. Fig 3b described the five grades of industrial SO₂ emissions, which indicated the spatial variations of industrial SO₂ emissions. And, Fig 4 showed the area ratios of these four types (Fig 4a) and five grades (Fig 4b) in China. On the whole, we can find that the growth of industrial SO₂ emissions was mostly distributed in 6.32% of China's total areas (Figs 3a and 4a). Specifically, two types (including high-growth

type and moderate-growth type) with relatively rapid growth, accounting for 1.35% of the national area, were mainly distributed in coastal areas and some metropolitan areas, including Chongqing and provincial capital cities. While, the other two types reflecting time variations of industrial SO₂ emissions, including no-obvious-growth type and low-growth type, which occupy 93.68% and 4.97% of the total national areas respectively, were located in the Western and Northeastern regions mainly. As for spatial variations, there existed a similar variations pattern. The low and relatively-low grade of industrial SO₂ emissions were mainly distributed in the Western region, covering 88.97% and 8.60% of the total national land, respectively (Figs 3b and 4b). Moreover, the high, relatively-high and medium grades accounted for 0.20%, 0.64%, 1.59% of the total national land, respectively, mainly distributing in the coastal and Central areas and Sichuan-Chongqing.

Spatiotemporal dynamics of industrial SO₂ emissions at regional scale. Fig 5 described the areal percentage of each type and each grade in China's four regions. According to Fig 5a, the high-growth type was mostly distributed in the Western region and Central region, occupying 62.47% and 25.17% of the total areas of that type, respectively. The moderate-growth and low-growth types were comparatively evenly located in China's Western region, Central region and Eastern region. While, the no-obvious-growth type was concentrated in the Western region mainly, covering 73.31% of the total areas of that type. Summarily, the high-growth of the industrial SO₂ emissions was mostly located in the Western region, followed by Central region, and the no-obvious-growth was mainly located in the Western region. Both the high-growth and no-obvious-growth of the industrial SO₂ emissions accounted for a large share in the western region, partly due to the large size of this region. Additionally, it is notable that the distribution of these four types in the Northeastern region was relatively small. This probably resulted from its relatively small size. As for the areal percentage of each grade, 38.57% of the high grade was distributed in Eastern region, 30.82% was located in Western region, 23.46% in Central region and the rest was located in Northeastern region (Fig 5b). The relatively-high grade was largely distributed in Eastern region where accounted for 52.82% of the total areas of this grade. While, 76.12% of the low grade was located in the Western region, with a fairly small proportion distributed in the Eastern, Central, and Northeastern regions. Similar to the four types, the proportions of the five grades of industrial SO₂ emissions in the Northeastern region were all relatively low. In summary, the high grade of industrial SO₂ emissions was mostly concentrated in the Eastern and Western regions, while the low grade was mainly located in the Western region.

Spatiotemporal dynamics of industrial SO₂ emissions at urban agglomeration scale. The representative six urban agglomerations covered 7.68% land area of this country, but contributed 35.33% of China's industrial SO₂ emissions for 1997–2013. In terms of the percentage of the total areas, 88.55% of Beijing-Tianjin-Tangshan and 86.17% of Middle south of Liaoning showed a no-obvious-growth type (Fig 6a). The growth of industrial SO₂ emissions was 21.32% in Pearl River Delta and 17.01% in Shanghai-Nanjing-Hangzhou presented a low-growth type, whereas 7.86% in Shanghai-Nanjing-Hangzhou and 6.41% in Pearl River Delta described a moderate-growth type. Besides, Shandong Peninsula should be paid much more attention to, because the areal percentage of high-growth type in this urban agglomeration was the biggest, reaching 1.27 percent. To sum up, the high-growth type of industrial SO₂ emissions was mainly located in Shandong Peninsula, while Beijing-Tianjin-Tangshan and Middle south of Liaoning showed a no-obvious-growth variation. Moreover, the low grade of industrial SO₂ emissions in Middle south of Liaoning and Beijing-Tianjin-Tangshan were 66.79% and 58.10%, respectively (Fig 6b). In addition, 3.27% in the Shanghai-Nanjing-Hangzhou showed a high grade and 10.76% presented a relatively-high grade. 2.43% of Shandong Peninsula presented a high grade and 4.54% showed a relatively-high grade. Summarily, the high grade of industrial SO₂

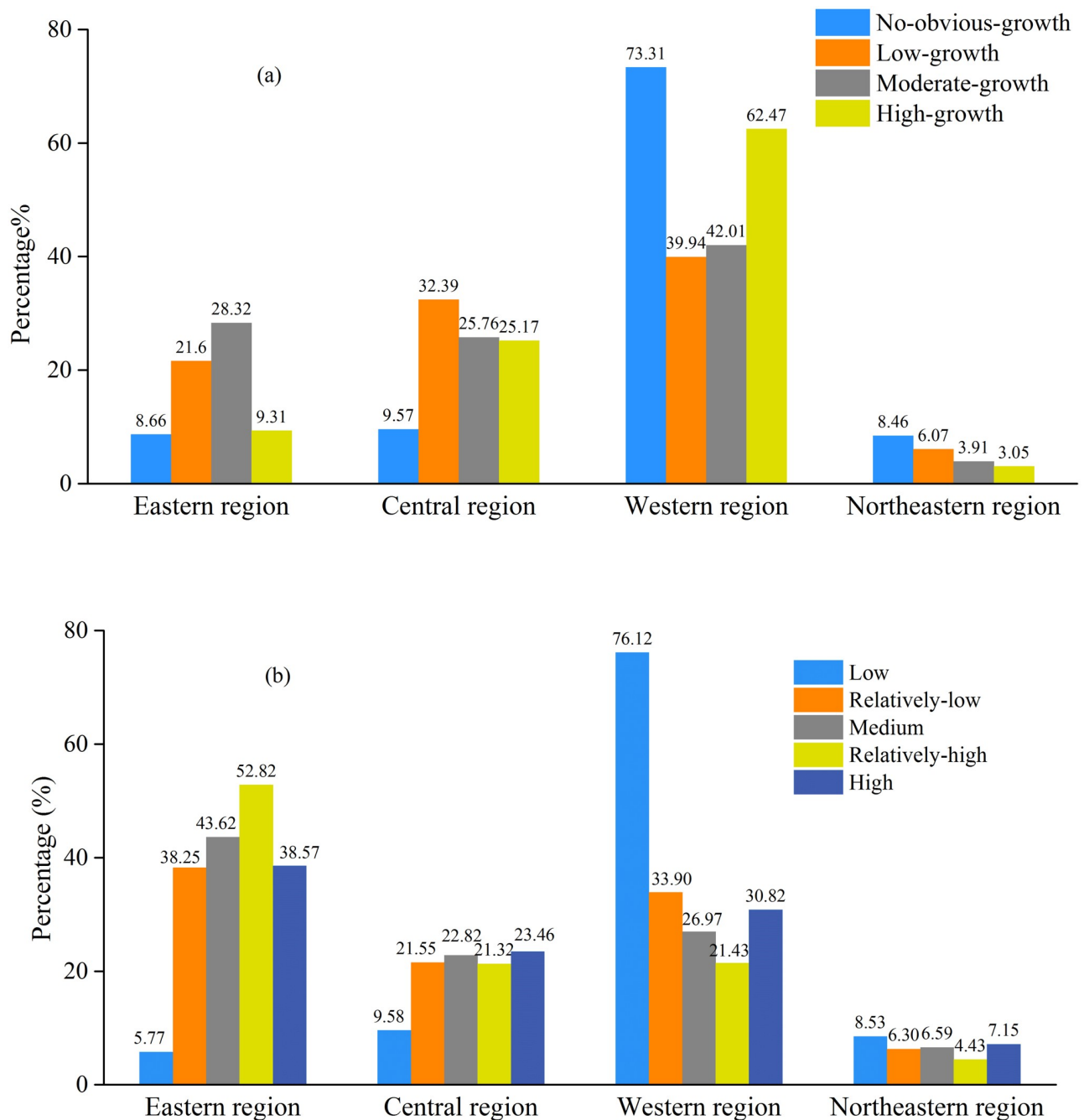


Fig 5. Areal percentage of each type (a) and each grade (b) in the four regions.

<https://doi.org/10.1371/journal.pone.0238696.g005>

emissions was concentrated in Shanghai-Nanjing-Hangzhou and Shandong Peninsula, while Middle south of Liaoning and Beijing-Tianjin-Tangshan presented a low grade.

Discussion

Accuracy evaluation of industrial SO₂ emissions estimation

Since we used the provincial statistical data to estimate the industrial SO₂ emissions, it is reasonable and reliable to assess the accuracy of the estimation models utilizing the industrial SO₂

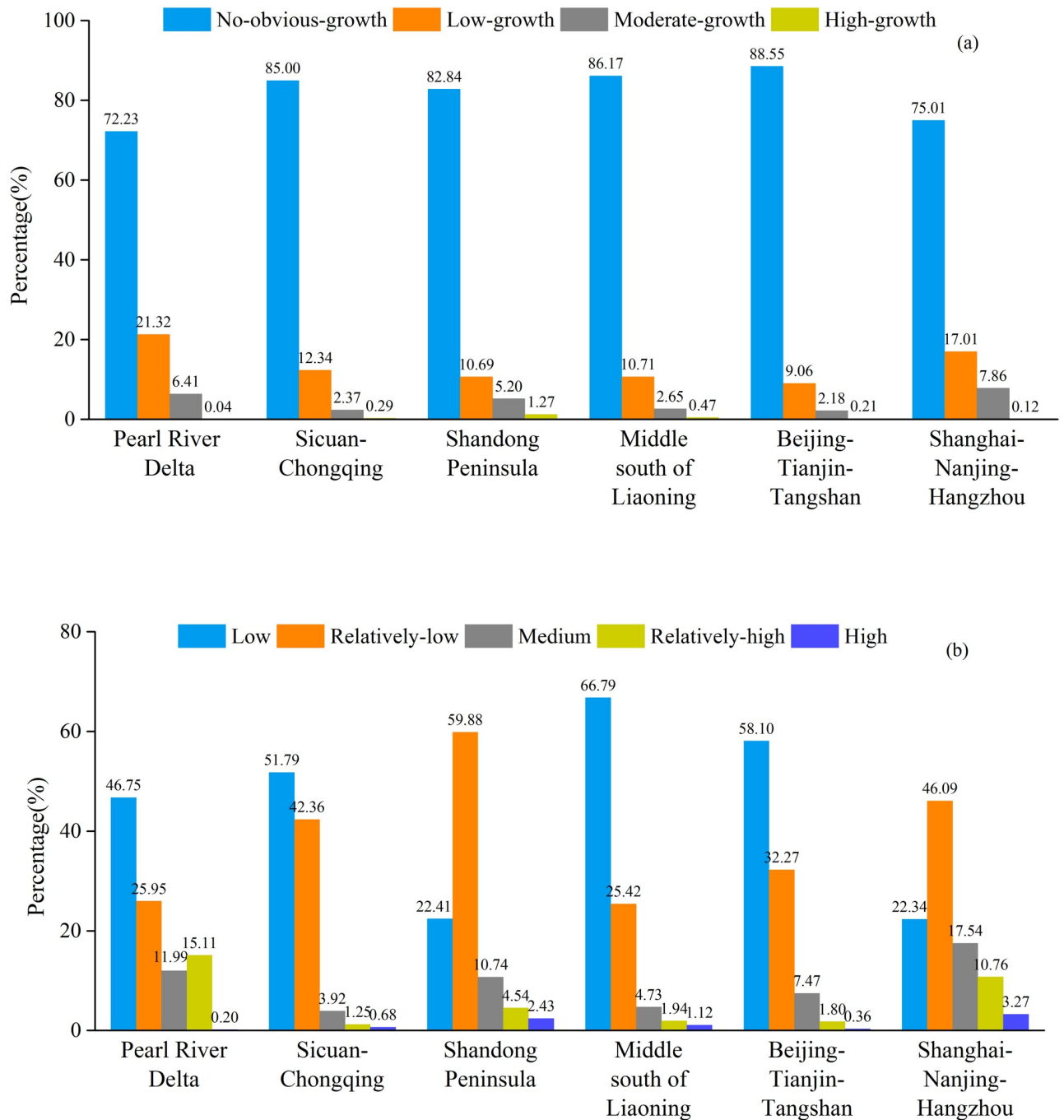


Fig 6. Areal percentage of each type (a) and each grade (b) within the six urban agglomerations.

<https://doi.org/10.1371/journal.pone.0238696.g006>

emission data at the prefectural level. Based on data availability, statistical industrial SO₂ emissions of 263 cities were selected to validate the estimated industrial SO₂ emissions in 2003, 2004, 2008, 2009, 2012 and 2013. Accordingly, two indicators, R² and RE were calculated to reflect the accuracy results (Fig 7).

It can be found that the minimum coefficient of determination (R²), was approximately 0.58, and all the other R² values were higher than 0.6. Additionally, the figure also reflected

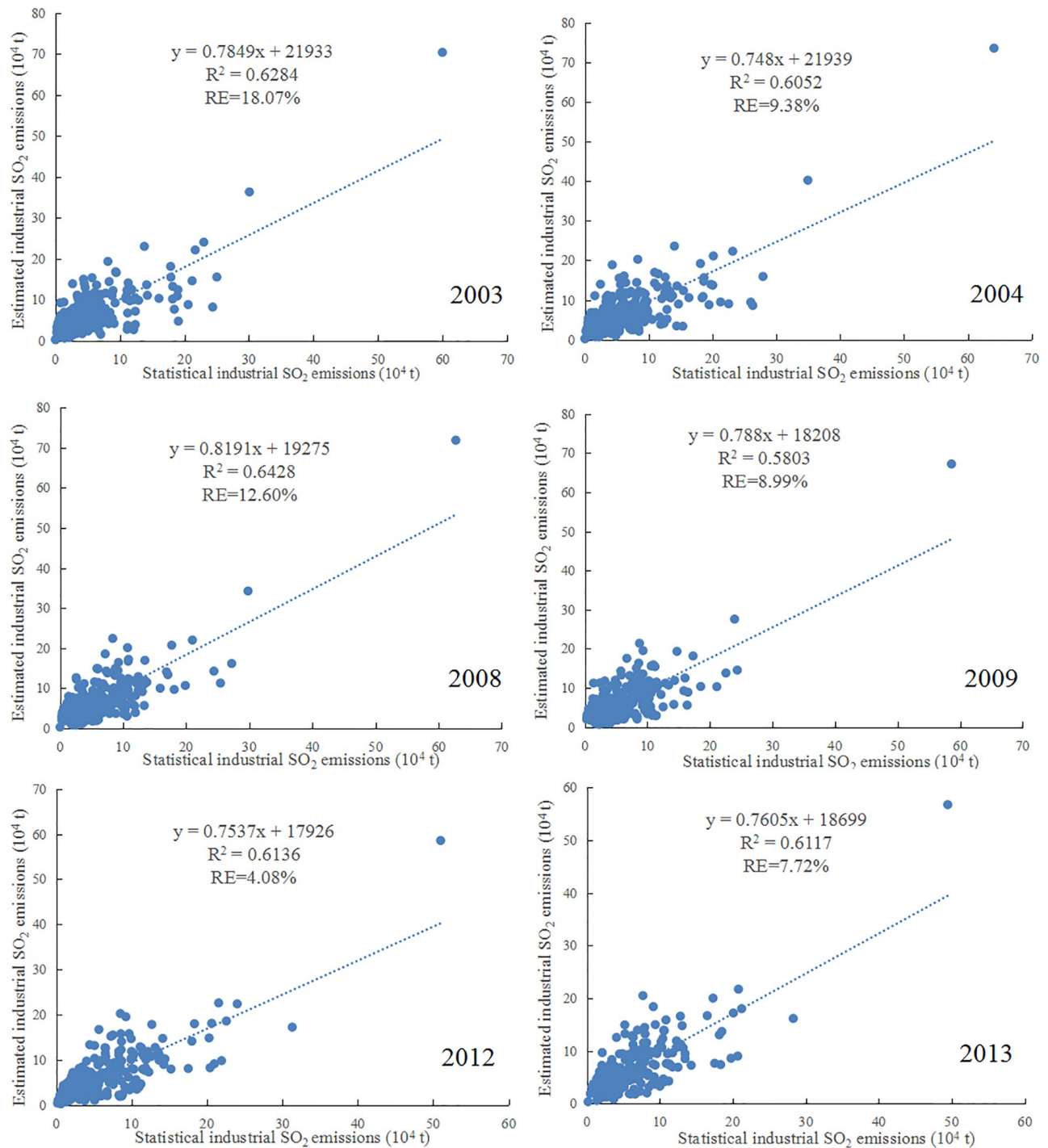


Fig 7. Validation scatters between the estimated and statistical industrial SO₂ emissions.

<https://doi.org/10.1371/journal.pone.0238696.g007>

that the RE was 18.07% for 2003, 9.38% for 2004, 12.60% for 2008, 8.99% for 2009, 4.08% for 2012 and 7.72% for 2013, respectively. In other words, the maximum relative error (RE) was 18.07%, and most of the RE values were lower than 10 percent. The results of our study are acceptable in comparison with the previous researches [49, 50, 57, 59]. Ji et al. [49] estimated

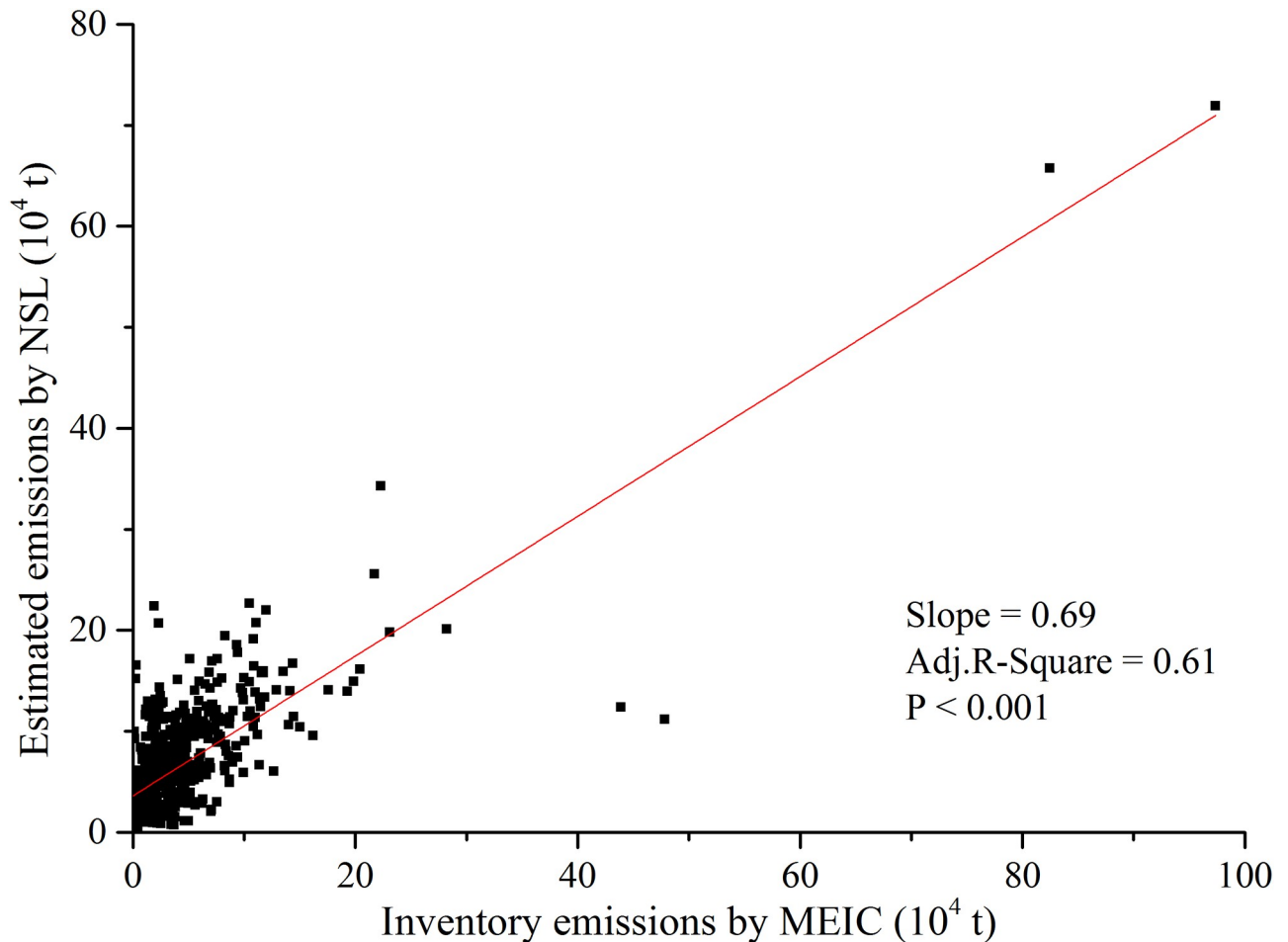


Fig 8. Comparison between inventory emissions by MEIC and estimated emissions by NSL at the prefectural level. Data in years of 2008, 2010; 712 samples.

<https://doi.org/10.1371/journal.pone.0238696.g008>

China's PM₁₀ emissions using DMSP-OLS data, the estimation accuracy was validated by city-level statistical PM₁₀ emissions for 1995, 2000 and 2005, and the R² were 0.5217, 0.5437, and 0.5158, respectively. Zhao et al. [57] employed nighttime light datasets to simulate urban residential CO₂ emissions in China, and the maximum RE is 23.084%, the average absolute value of RE is 12.84%.

Moreover, in order to further evaluate the reliability of the NSL-based estimation results, we compared the estimated industrial SO₂ emissions with the Multi-resolution Emission Inventory for China (MEIC) database, which is a bottom-up emission inventory framework developed and maintained by Tsinghua University [60]. The emission inventory utilized in this article was downloaded from <http://www.meicmodel.org/dataset-mix.html>, where it is freely available for non-commercial purposes. Based on the availability of data, we compared the emissions of 356 prefecture level cities in 2008 and 2010. And the comparison results are shown in Fig 8. It can be discovered that the Adj.R-Square reached 0.61, with the significance at the 0.001 level. In other words, the DMSP-OLS NSL-based estimation results are acceptable compared with the emissions estimated by other approach.

Therefore, the accuracy evaluation results show that the industrial SO₂ emissions in China can be modeled by NSL data. In addition, it is worth noting that the inconsistency of statistical

criterion between provincial and municipal statistical data affects the simulation accuracy to a certain extent. We believe that the simulation accuracy will be improved if the availability and reliability of statistical data was enhanced.

Suggestions for industrial SO₂ emissions reduction

In order to reduce China's industrial SO₂ emissions to achieve the sustainable development of social economy, more efforts should be made to adjust, optimize and upgrade the industrial structures and enhance the energy utilizing efficiency. Considering the great differences in economic development among regions, the Chinese government should adopt differentiated mitigation strategies for different regions. For the Eastern and Central regions with higher levels of economic development, the reduction strategies of industrial SO₂ emissions should focus on adjusting and optimizing the industrial structure. High energy-consuming industries, such as the manufactures of chemical materials and products, metal smelting and calendering, production and supply of electric power and hot power should be close down or reformed through improving the manufacturing technology, technologic process and production equipment. At the same time, the government should vigorously develop the low-energy-consuming industries such as information services, financial insurance, Internet and tourism, actively promote industrial upgrading and change the situation of heavy industrial structure. Due to the Western and Northeastern regions are mainly dominated by energy-related and heavy industries, the reduction strategies of industrial SO₂ emissions should put more emphasis on the energy structure optimizations and energy efficiency improvement in these two regions. Since these two regions are all at the initial stages of China's economic development, it seems to be unfeasible and unrealistic for them to alter the coal-based energy consumption structure at the present stage. But, reducing industrial SO₂ emissions through improving energy efficiency and the performance of flue gas desulfurization facilities seems to be more feasible and effective, in a short-term period. In a long run, the Western and Northeastern regions with abundant wind and solar energy resources, can gradually develop and utilize these renewable energy sources to replace the coal-dominated energy structure. Besides, related laws and policies should be timely formulated for facilitating the industrial SO₂ emissions reduction in the whole country. For example, extra taxation should be imposed on the industries with high industrial SO₂ emissions in the Eastern and Central regions. While, in the Western and Northeast regions, tax breaks, loan concessions and fiscal subsidy could be granted to the industries using renewable energies or developing advanced technologies for lower industrial SO₂ emissions. Additionally, for the six representative urban agglomerations, industrial SO₂ emissions in Shandong Peninsula was not only higher in grade, but also more obvious in increasing trend. Therefore, more attention should be paid to industrial SO₂ emission reduction of this urban agglomerations.

Conclusions

In order to cope with the industrial SO₂ pollution problems in China, this study explored the spatiotemporal dynamics of industrial SO₂ emissions from 1997 to 2013, and put forward relevant suggestions on industrial SO₂ emission mitigation. On the basis of proving that there was a positive correlation between the DMSP-OLS stable lights and industrial SO₂ emissions, we tried to utilize NSL data to simulate industrial SO₂ emissions. By building linear regression models, we estimated China's industrial SO₂ emissions at 1 km resolution from 1997 to 2013, and evaluated the NSL-based estimation results. The accuracy evaluation results showed that the NSL-based estimation results were acceptable. Eventually, we investigated the spatiotemporal dynamic changes of China's industrial SO₂ emissions from three different scales, and

proposed corresponding reduction suggestions for industrial SO₂ emissions. The estimation results apparently exhibited that the distribution of industrial SO₂ emissions differed greatly during the investigation period. Specifically, the high growth type of industrial SO₂ emissions was mainly distributed in the Western region, Central region, and Shandong Peninsula, while the no-obvious-growth type was concentrated in Western region, Beijing-Tianjin-Tangshan and Middle south of Liaoning. And, the high grade was concentrated in Eastern China, Western region, Shanghai-Nanjing-Hangzhou, and Shandong Peninsula, while the low grade mostly located in Western region, Middle south of Liaoning and Beijing-Tianjin-Tangshan. Seeing that the spatio-temporal changes of industrial SO₂ emissions in different regions varied greatly, reduction strategies in Eastern China and Central China should put emphasis on industrial restructuring, while in Western China and Northeastern China, more attentions should be paid to optimize the regional energy structure and improve the energy utilization efficiency.

The findings of our research can not only contribute to comprehensively comprehend the regional differences of spatiotemporal industrial SO₂ emission dynamics at the multiple scales, but also give some scientific references for formulating feasible industrial SO₂ emission reduction policies. But, there are limitations that are worth mentioning. First, the provincial statistical industrial SO₂ emissions which were used to model the distributions of China's industrial SO₂ emissions, may be distorted due to the inconsistent statistical caliber and artificial error. Second, although the linear regression model established in this study based on NSL data, was proved to be an effective means to estimate industrial SO₂ emissions, there indeed exist errors with NSL data as the only index in the simulation models. In order to improve the simulation accuracy, other indicators (such as economic development, industrial structure, land use data, etc.) should also be taken into account when establishing estimation models. In addition, other simulation methods (like panel data analysis, exponential model, and logarithmic model, etc.) should also be tried and compared to determine which model will be better. Third, as for the spatiotemporal dynamics of industrial SO₂ emissions varied greatly from different regions, the driving mechanism of industrial SO₂ emissions in China should be detected in a follow-up study.

Supporting information

S1 File. Original data of industrial SO₂ emissions of 31 provinces in China from 1997 to 2013.

(XLS)

S2 File. Original data of industrial SO₂ emissions of 263 cities in China in 2003, 2004, 2008, 2009, 2012, and 2013.

(XLS)

Author Contributions

Conceptualization: Yanlin Yue, Guangxing Ji.

Data curation: Li Tian.

Formal analysis: Yanlin Yue, Jincai Zhao.

Methodology: Yanlin Yue, Li Tian.

Writing – original draft: Yanlin Yue.

Writing – review & editing: Yanlin Yue, Zheng Wang, Zhizhu Lai, Haibin Xia.

References

1. Jeong JI, Park RJ. Effects of the meteorological variability on regional air quality in East Asia. *Atmospheric Environment*. 2013; 69: 46–55. <https://doi.org/10.1016/j.atmosenv.2012.11.061>
2. Xu WJ, Li JX, Zhang WH, Wang ZX, Wu JJ, Ge XJ, et al. Emission of sulfur dioxide from polyurethane foam and respiratory health effects. *Environmental Pollution*. 2018; 242: 90–97. <https://doi.org/10.1016/j.envpol.2018.06.089>
3. Grandey BS, Yeo LK, Lee HH, Wang C. The Equilibrium Climate Response to Sulfur Dioxide and Carbonaceous Aerosol Emissions from East and Southeast Asia. *Geophysical Research Letters*. 2018; 45(20). <https://doi.org/10.1029/2018gl080127>
4. Likens GE, Bormann FH. Acid rain: a serious regional environmental problem. *Science*. 1974; 184(4142): 1176–1179. <https://doi.org/10.1126/science.184.4142.1176>
5. Streets DG, Akimoto H, Ny OKT. Sulfur dioxide emissions in Asia in the period 1985–1997. *Atmospheric Environment*. 2000; 34(26): 4413–4424. [https://doi.org/10.1016/S1352-2310\(00\)00187-4](https://doi.org/10.1016/S1352-2310(00)00187-4)
6. Smith SJ, Pitcher H, Wigley TML. Future Sulfur Dioxide Emissions. *Climatic Change*. 2005; 73(3): 267–318. <https://doi.org/10.1007/s10584-005-6887-y>
7. Huang M, Carmichael GR, Spak SN, Adhikary B, Kulkarni S, Cheng Y, et al. Multi-scale modeling study of the source contributions to near-surface ozone and sulfur oxides levels over California during the ARCTAS-CARB period. *Atmospheric Chemistry and Physics*. 2011; 11(7): 3173–3194. <https://doi.org/10.5194/acp-11-3173-2011>
8. Ge C, Wang J, Carn S, Yang K, Ginoux P, Krotkov N. Satellite-based global volcanic SO₂ emissions and sulfate direct radiative forcing during 2005–2012. *Journal of Geophysical Research: Atmospheres*. 2016; 121(7): 3446–3464. <https://doi.org/10.1002/2015JD023134>
9. Hoesly RM, Smith SJ, Feng L, Klimont Z, Janssens-Maenhout G, Pitkanen T, et al. Historical (1750–2014) anthropogenic emissions of reactive gases and aerosols from the Community Emissions Data System (CEDS). *Geoscientific Model Development*. 2018; 11(1): 369–408. <https://doi.org/10.5194/gmd-11-369-2018>
10. Greenpeace India. Global SO₂ emission hotspot database: ranking the world's worst sources of SO₂ pollution [EB/OL]. <https://www.greenpeace.org/india/en/publication/3951/global-so2-emission-hotspots-database-ranking-the-worlds-worst-sources-of-so2-pollution-2/>, 2019-8-19.
11. Zhong QR, Shen HZ, Yun X, Chen YL, Ren YA, Xu HR, et al. Global Sulfur Dioxide Emissions and the Driving Forces. *Environmental Science & Technology*. 2020; 54(11): 6508–6517. <https://doi.org/10.1021/acs.est.9b07696>
12. Meng B, Xue JJ, Feng KS, Guan DB, Fu X. China's inter-regional spillover of carbon emissions and domestic supply chains. *Energy Policy*. 2013; 61: 1305–1321. <https://doi.org/10.1016/j.enpol.2013.05.108>
13. Xue JJ, Zhao ZX, Dai YD, Wang B. Annual Report on China's Low-Carbon Economic Development. Social Sciences Academic Press. 2012.
14. van der A RJ, Mijling B, Ding JY, Koukouli ME, Liu F, Li Q, et al. Cleaning up the air: effectiveness of air quality policy for SO₂ and NO_x emissions in China. *Atmospheric Chemistry and Physics*. 2017; 17(3): 1775–1789. <https://doi.org/10.5194/acp-17-1775-2017>
15. Ministry of Ecology and Environment, PRC. Bulletin of national environmental statistics (2015). [EB/OL]. <http://www.mee.gov.cn/hjzl/sthjzk/sthjtnb/201702/P020170223595802837498.pdf>, 2017-2-23.
16. Zhang Q, He KB, Huo H. Cleaning China's air. *Nature*. 2012; 484(7393): 161–162. <https://doi.org/10.1038/484161a>
17. Yuan R, Behrens P, Tukker A, Rodrigues JFD. Carbon overhead: The impact of the expansion in low-carbon electricity in China 2015–2040. *Energy Policy*. 2018; 119: 97–104. <https://doi.org/10.1016/j.enpol.2018.04.027>
18. The State Council, PRC. Circular of the State Council on Issuing the Three-year Action Plan for Blue Sky Defense War. [EB/OL]. http://www.gov.cn/zhengce/content/2018-07/03/content_5303158.htm, 2018-6-27.
19. Zeng BH, Wu T, Guo XX. Interprovincial trade, economic development and the impact on air quality in China. *Resources, Conservation and Recycling*. 2019; 142: 204–214. <https://doi.org/10.1016/j.resconrec.2018.12.002>
20. Ministry of Ecology and Environment, PRC. Background materials of China's Eco-environment Bulletin 2017. [EB/OL]. http://www.mee.gov.cn/gkml/sthjbgw/qt/201805/t20180531_442212.htm, 2018-5-31.
21. Lin MY, Oki T, Bengtsson M, Kanae S, Holloway T, Streets DG. Long-range transport of acidifying substances in East Asia-Part II: Source-receptor relationships. *Atmospheric Environment*. 2008; 42(24): 5956–5967. <https://doi.org/10.1016/j.atmosenv.2008.03.039>

22. Su SS, Li BG, Cui SY, Tao S. Sulfur Dioxide Emissions from Combustion in China: From 1990 to 2007. *Environmental Science & Technology*. 2011; 45(19): 8403–8410. <https://doi.org/10.1021/es201656f>
23. Zhang QL, Seto KC. Mapping urbanization dynamics at regional and global scales using multi-temporal DMSP/OLS nighttime light data. *Remote Sensing of Environment*. 2011; 115(9): 2320–2329. <https://doi.org/10.1016/j.rse.2011.04.032>
24. Ting MA, Zhou CH, Tao P, HAYNIE Susan, Fan JF. Quantitative estimation of urbanization dynamics using time series of DMSP/OLS nighttime light data: A comparative case study from China's cities. *Remote Sensing of Environment*. 2012; 124(124): 99–107. <https://doi.org/10.1016/j.rse.2012.04.018>
25. Li QT, Lu LL, Weng QH, Xie YH, Guo HD. Monitoring Urban Dynamics in the Southeast U.S.A. Using Time-Series DMSP/OLS Nightlight Imagery. *Remote Sensing*. 2016; 8(7): 578. <https://doi.org/10.3390/rs8070578>
26. Min Z, Cheng WM, Zhou CH, Li MC, Huang K, Nan W. Assessing Spatiotemporal Characteristics of Urbanization Dynamics in Southeast Asia Using Time Series of DMSP/OLS Nighttime Light Data. *Remote Sensing*. 2018; 10(1): 47. <https://doi.org/10.3390/rs10010047>
27. Amaral S, Monteiro AMV, Camara G, Quintanilha JA. DMSP/OLS night-time light imagery for urban population estimates in the Brazilian Amazon. *International Journal of Remote Sensing*. 2006; 27(5): 855–870. <https://doi.org/10.1080/01431160500181861>
28. Tripathi BR, Tiwari V, Pandey V, Elvidge C, Rawat JS, Sharma MP, et al. Estimation of Urban Population Dynamics using DMSP-OLS Night-time Lights Time Series Sensors Data. *Ieee Sensors Journal*. 2017; 17(4): 1013–1020. <https://doi.org/10.1109/JSEN.2016.2640181>
29. Li XM, Zhou WQ. Dasyymmetric mapping of urban population in China based on radiance corrected DMSP-OLS nighttime light and land cover data. *Science of the Total Environment*. 2018; 643(1): 1248–1256. <https://doi.org/10.1016/j.scitotenv.2018.06.244>
30. Yu SS, Zhang ZX, Liu F. Monitoring Population Evolution in China Using Time-Series DMSP/OLS Nightlight Imagery. *Remote Sensing*. 2018; 10(2): 194. <https://doi.org/10.3390/rs10020194>
31. Wu JS, Wang Z, Li WF, Peng J. Exploring factors affecting the relationship between light consumption and GDP based on DMSP/OLS nighttime satellite imagery. *Remote Sensing of Environment*. 2013; 134(7): 111–119. <https://doi.org/10.1016/j.rse.2013.03.001>
32. Doll CNH, Muller JP, Morley JG. Mapping regional economic activity from night-time light satellite imagery. *Ecological Economics*. 2006; 57(1): 75–92. <https://doi.org/10.1016/j.ecolecon.2005.03.007>
33. Yue WZ, Gao JB, Yang XC. Estimation of Gross Domestic Product Using Multi-Sensor Remote Sensing Data: A Case Study in Zhejiang Province, East China. *Remote Sensing*. 2014; 6(8): 7260–7275. <https://doi.org/10.3390/rs6087260>
34. Elvidge CD, Baugh KE, Kihn EA, Kroehl HW, Davis ER, Davis CW. Relation between satellite observed visible-near infrared emissions, population, economic activity and electric power consumption. *International Journal of Remote Sensing*. 1997; 18(6): 1373–1379. <https://doi.org/10.1080/014311697218485>
35. Zhao N, Ghosh T, Samson EL. Mapping spatio-temporal changes of Chinese electric power consumption using night-time imagery. *International Journal of Remote Sensing*. 2012; 33(20): 6304–6320. <https://doi.org/10.1080/01431161.2012.684076>
36. He CY, Ma Q, Liu ZF, Zhang QF. Modeling the spatiotemporal dynamics of electric power consumption in Mainland China using saturation-corrected DMSP/OLS nighttime stable light data. *International Journal of Digital Earth*. 2014; 7(12): 993–1014. <https://doi.org/10.1080/17538947.2013.822026>
37. Shi KF, Chen Y, Yu BL, Xu TB, Yang CS, Li LY, et al. Detecting spatiotemporal dynamics of global electric power consumption using DMSP-OLS nighttime stable light data. *Applied Energy*. 2016; 184: 450–463. <https://doi.org/10.1016/j.apenergy.2016.10.032>
38. Letu H, Hara M, Yagi H, Naoki K, Tana G, Nishio F, et al. Estimating energy consumption from night-time DMPS/OLS imagery after correcting for saturation effects. *International Journal of Remote Sensing*. 2010; 31(16): 4443–4458. <https://doi.org/10.1080/01431160903277464>
39. Yue YL, Tian L, Yue Q, Wang Z. Spatiotemporal Variations in Energy Consumption and Their Influencing Factors in China Based on the Integration of the DMSP-OLS and NPP-VIIRS Nighttime Light Datasets. *Remote Sensing*. 2020; 12(7): 1151. <https://doi.org/10.3390/rs12071151>
40. Doll CH, Muller JP, Elvidge CD. Night-time imagery as a tool for global mapping of socioeconomic parameters and greenhouse gas emissions. *AMBIO: A Journal of the Human Environment*. 2000; 29(3): 157–162. <https://doi.org/10.1579/0044-7447-29.3.157>
41. Ghosh T, Elvidge CD, Sutton PC, Baugh KE, Ziskin D, Tuttle BT. Creating a Global Grid of Distributed Fossil Fuel CO₂ Emissions from Nighttime Satellite Imagery. *Energies*. 2010; 3(12): 1895–1913. <https://doi.org/10.3390/en3121895>
42. Meng L, Graus W, Worrell E, Bo H. Estimating CO₂ (carbon dioxide) emissions at urban scales by DMSP/OLS (Defense Meteorological Satellite Program's Operational Linescan System) nighttime light

- imagery: Methodological challenges and a case study for China. *Energy*. 2014; 71: 468–478. <https://doi.org/10.1016/j.energy.2014.04.103>
43. Cui XL, Lei YT, Zhang F, Zhang XY, Wu F. Mapping spatiotemporal variations of CO₂ (carbon dioxide) emissions using nighttime light data in Guangdong Province. *Physics and Chemistry of the Earth, Parts A/B/C*. 2019; 110: 89–98. <https://doi.org/10.1016/j.pce.2019.01.007>
 44. Liu XP, Ou JP, Wang SJ, Li X, Yan YC, Jiao LM, et al. Estimating spatiotemporal variations of city-level energy-related CO₂ emissions: An improved disaggregating model based on vegetation adjusted nighttime light data. *Journal of Cleaner Production*. 2018; 177: 101–114. <https://doi.org/10.1016/j.jclepro.2017.12.197>
 45. Li RY, Liu XN, Li XQ. Estimation of the PM_{2.5} Pollution Levels in Beijing Based on Nighttime Light Data from the Defense Meteorological Satellite Program-Operational Linescan System. *Atmosphere*. 2015; 6(5): 607–622. <https://doi.org/10.3390/atmos6050607>
 46. Xu Z, Xia XP, Liu XN, Qian ZG. Combining DMSP/OLS Nighttime Light with Echo State Network for Prediction of Daily PM_{2.5} Average Concentrations in Shanghai, China. *Atmosphere*. 2015; 6(10): 1507–1520. <https://doi.org/10.3390/atmos6101507>
 47. Toenges-Schuller N, Stein O, Rohrer F, Wahner A, Richter A, Burrows JP, et al. Global distribution pattern of anthropogenic nitrogen oxide emissions: Correlation analysis of satellite measurements and model calculations. *Journal of Geophysical Research*. 2006; 111(D5). <https://doi.org/10.1029/2005JD006068>
 48. Jiang JH, Zhang JY, Zhang YW, Zhang CL, Tian GM. Estimating nitrogen oxides emissions at city scale in China with a nightlight remote sensing model. *Science of the Total Environment*. 2016; 544: 1119–1127. <https://doi.org/10.1016/j.scitotenv.2015.11.113>
 49. Ji GX, Zhao JC, Yang X, Yue YL, Wang Z. Exploring China's 21-year PM₁₀ emissions spatiotemporal variations by DMSP-OLS nighttime stable light data. *Atmospheric Environment*. 2018; 191: 132–141. <https://doi.org/10.1016/j.atmosenv.2018.07.045>
 50. Ji GX, Tian L, Zhao JC, Yue YL, Wang Z. Detecting spatiotemporal dynamics of PM_{2.5} emission data in China using DMSP-OLS nighttime stable light data. *Journal of Cleaner Production*. 2019; 209: 363–370. <https://doi.org/10.1016/j.jclepro.2018.10.285>
 51. Fioletov VE, McLinden CA, Krotkov N, Li C, Joiner J, Theys N, et al. A global catalogue of large SO₂ sources and emissions derived from the Ozone Monitoring Instrument. *Atmospheric Chemistry and Physics Discussions*. 2016: 1–45. <https://doi.org/10.5194/acp-2016-417>
 52. Brandt P, Nuhn A, Lange M, Möllmer J, Weingart O, Janiak C. Metal–Organic Frameworks with Potential Application for SO₂ Separation and Flue Gas Desulfurization. *ACS Applied Materials & Interfaces*. 2019; 11(19): 17350–17358. <https://doi.org/10.1021/acsami.9b00029>
 53. Han XD, Zhou Y, Wang SX, Liu R, Yao Y. GDP Spatialization in China Based on Nighttime Imagery. *Journal of Geo-information Science*. 2012; 14(1): 128–136. <https://doi.org/10.3724/SP.J.1047.2012.00128>
 54. Li ZG, Hu DY, Li JH, Cen J. Simulation and spatialization of GDP in poverty areas based on night light imagery. *Remote Sensing for Land and Resources*. 2016; 28(2): 168–174. <https://doi.org/10.6046/gtzyyg.2016.02.26>
 55. Huang M, Crawford JH, Carmichael GR, Santanello JA, Kumar SV, Stauffer RM, et al. Impact of Aerosols From Urban and Shipping Emission Sources on Terrestrial Carbon Uptake and Evapotranspiration: A Case Study in East Asia. *Journal of Geophysical Research: Atmospheres*. 2020; 125(2). <https://doi.org/10.1029/2019JD030818>
 56. Su YX, Chen XZ, Li Y, Liao JS, Ye YY, Zhang HG, et al. China's 19-year city-level carbon emissions of energy consumptions, driving forces and regionalized mitigation guidelines. *Renewable and Sustainable Energy Reviews*. 2014; 35: 231–243. <https://doi.org/10.1016/j.rser.2014.04.015>
 57. Zhao JC, Ji GX, Yue YL, Lai ZZ, Chen YL, Yang DY, et al. Spatio-temporal dynamics of urban residential CO₂ emissions and their driving forces in China using the integrated two nighttime light datasets. *Applied Energy*. 2019; 235: 612–624. <https://doi.org/10.1016/j.apenergy.2018.09.180>
 58. Xie HL, Zou JL, Peng XL. Spatial-temporal Difference Analysis of Cultivated Land Use Intensity Based on Emery in Poyang Lake Eco-economic Zone. *Acta Geographica Sinica*. 2012; 67(7): 889–902. <https://doi.org/10.11821/xb201207003>
 59. He CY, Ma Q, Liu ZF, Zhang QF. Modeling the spatiotemporal dynamics of electric power consumption in Mainland China using saturation-corrected DMSP/OLS nighttime stable light data. *International Journal of Digital Earth*. 2013; 7(12): 993–1014. <https://doi.org/10.1080/17538947.2013.822026>
 60. Li M, Zhang Q, Kurokawa J, Woo J, He K, Lu Z, et al. MIX: a mosaic Asian anthropogenic emission inventory under the international collaboration framework of the MICS-Asia and HTAP. *Atmospheric Chemistry and Physics*. 2017; 17(2): 935–963. <https://doi.org/10.5194/acp-17-935-2017>

© 2020 Yue et al. This is an open access article distributed under the terms of the Creative Commons Attribution License:

<http://creativecommons.org/licenses/by/4.0/>(the “License”), which permits unrestricted use, distribution, and reproduction in any medium, provided the original author and source are credited. Notwithstanding the ProQuest Terms and Conditions, you may use this content in accordance with the terms of the License.